

INTRODUCTION

MIT Lincoln Laboratory built two identical space payloads that will be hosted on the Japanese QZS-6 and QZS-7 satellites. The payloads are part of a collaborative effort between the United States and Japan to augment space domain awareness of objects in or near geosynchronous orbit (GEO). The payload mass budget and thermal environment for QZS-HP are both challenging, which led to the choice of silicon carbide (SiC) as the system's mirror material. The high stiffness-to-weight ratio allows for a very low mass mirror that can resist the forces and moments that tend to distort the mirror due to bearing misalignments. The low thermal expansion and high thermal conductivity minimize thermal gradients that would cause distortion of the mirror surface in a changing thermal environment. The MIT LL payload team selected the SuperSiC[®]-SP material produced by Entegris for the mirror substrates. The material has the desired properties and can be produced to near net shape with the desired rib structure, but requires a cladding on the optical surface to achieve the surface figure and roughness required for the mirror. The CVD SiC is Entegris' standard choice for this cladding due to its similarity with the substrate material as well as its polishability. The introduction of this material, however, has the potential to change the mirror flatness over temperature, even with small differences in thermal expansion between the cladding and the substrate. Since the mirror will have to operate on orbit at temperatures as low as -40°C, this concerned the MIT LL payload team enough to perform risk reduction testing in advance of the flight mirror fabrication.

MIT Lincoln Laboratory designed the optical payload to enable space situational awareness for the Japanese QZS-6 and QZS-7 GEO GPS satellites.

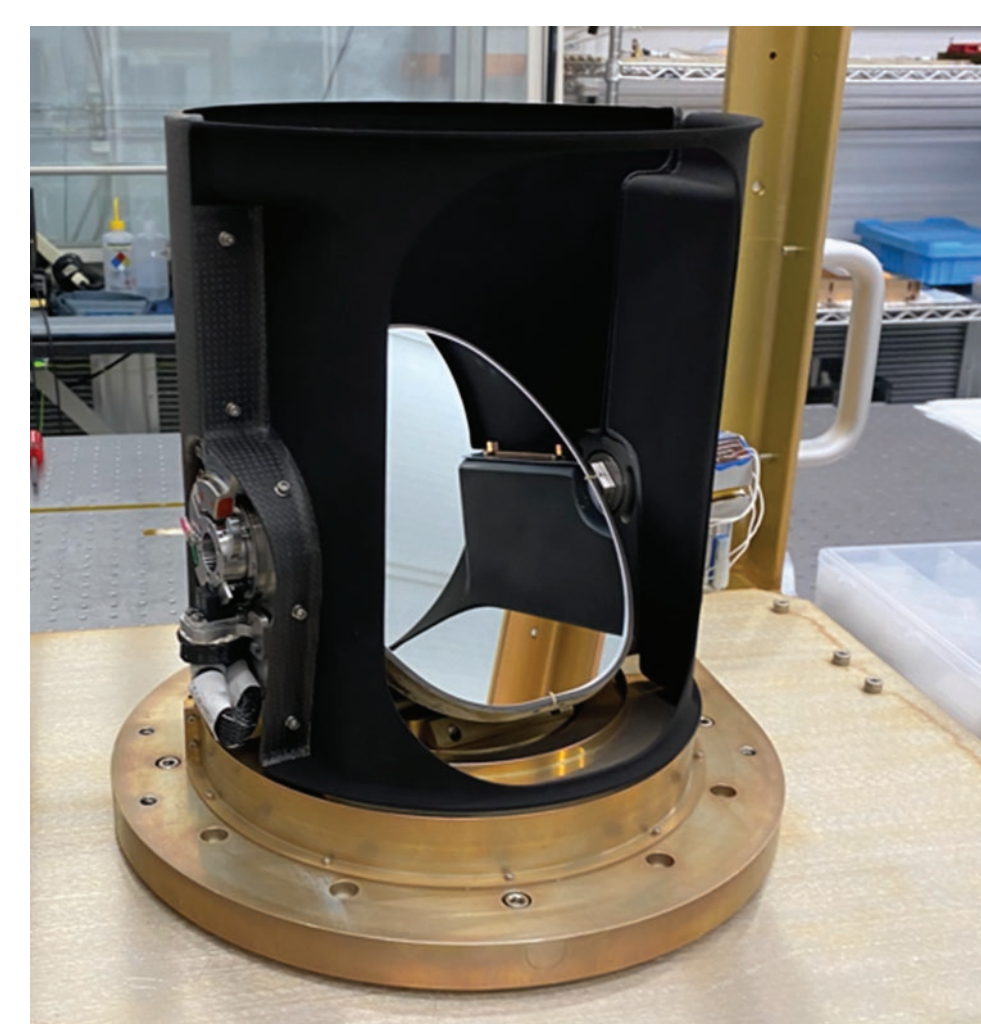


Figure 1. Two-axis gimbal mounted mirror assembly.

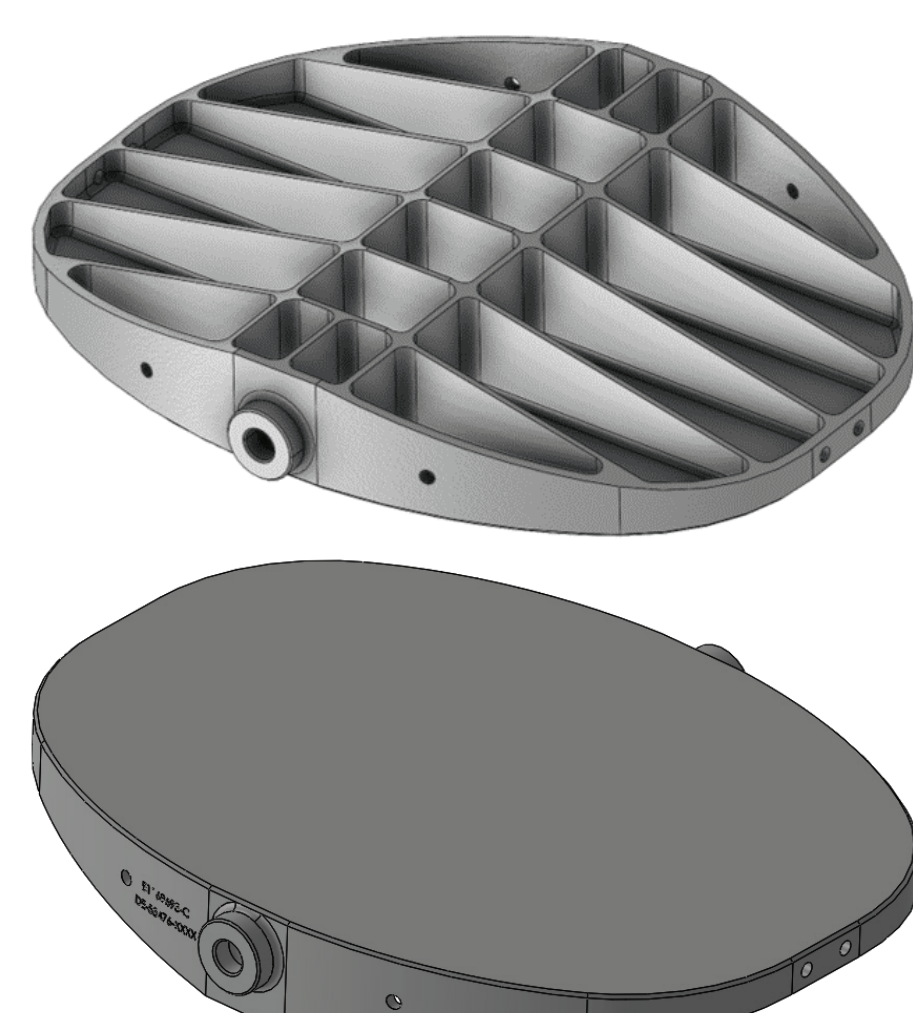


Figure 2. Entegris SUPERSiC-SP mirror isometric views.

Mirror Fabrication

The QZSS-HP mirrors were designed and manufactured in SiC supplied by Entegris, Inc. It is well known that there are several methods for making SiC and each creates products with properties unique to that method. Figure 3 illustrates the implied thermal mechanical trades for several common manufacturing processes. The Entegris SUPERSiC process is unique among the SiC manufacturing options in that it begins with a block of purified synthetic graphite. This specialty material is designed to be converted into SiC, but is similar to other synthetic graphite in its ability to be easily machined into structures with tight tolerances using standard carbide tooling and dry milling equipment. The particle size and stiffness of the graphite allow for stiffening structures to be designed down to 0.020" thick with high aspect ratio. Such net-shaped parts are then converted to 100% 3C (Beta) SiC in a high-temperature Chemical Vapor Conversion process. Individual carbon atoms within the structure are replaced in the process with single Si atoms. Since no excess Si can be formed, the process yields products to the right side of the carbon (C) percentage, which is dominated by the beta phase.

To allow for optical surfacing, a 100% dense SiC coating was applied to the mirror surface. However, the addition of the cladding gives rise to a bi-material effect, leaving the mirror subject to deformation over temperature as a result of the small difference in thermal coefficient between the SUPERSiC-SP base and the CVD SiC coating. The team designed thin mechanical coupons as part of the test plan for use in measuring the induced deformation and to determine the CTE difference.

Figure of Merit Comparison

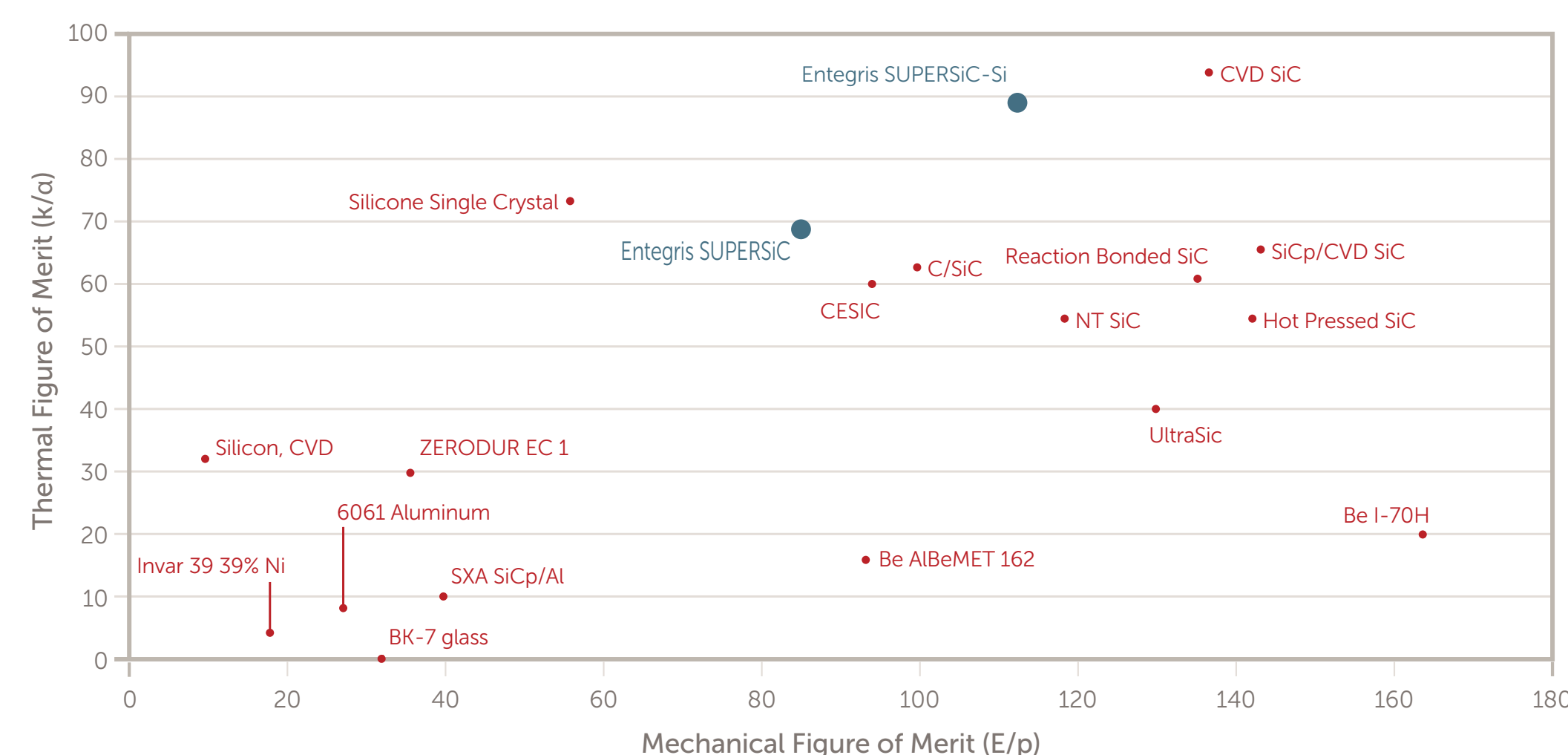


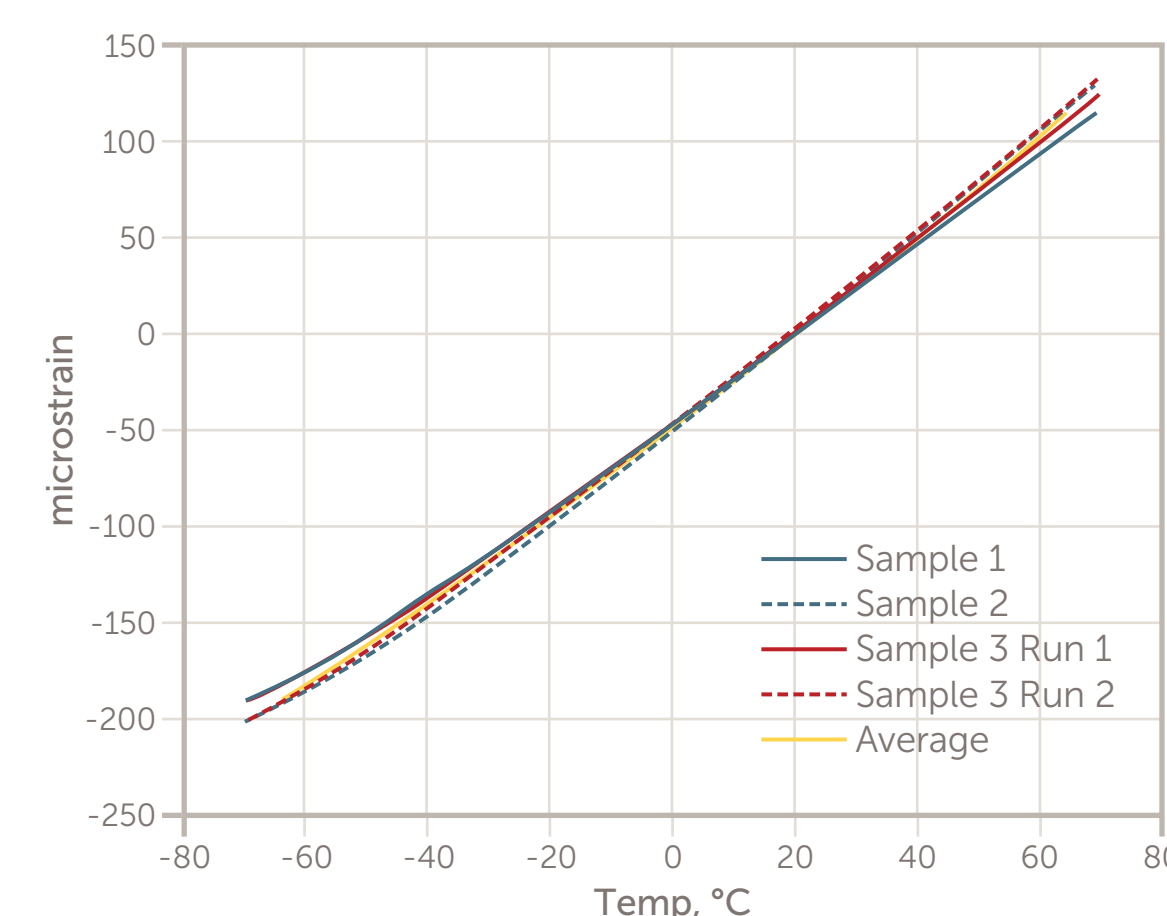
Figure 3. Optics materials trades: specific stiffness vs. thermal figure of merit.

METHODS

CTE Measurements of SuperSiC-SP

Test bars were tested using a Thermo-mechanical Analyzer (TMA450EM, TA Instruments). Entegris provided twelve bars, each approximately 0.25 inch square and 0.775 inch long. Of these twelve bars, three with flat parallel end conditions were chosen to provide the lowest noise measurements. Using the TMA, the thermal strain of the bars was measured over the temperature range from -70°C to 70°C. Some small differences were noticed between the bars that were similar to repeating the measurement on a single bar. Figure 4 shows the thermal strain plotted for the three samples, including a repeat measurement on the third. The raw thermal strains were averaged over these four measurements and then fit with a second-order polynomial over the range of -65°C to 65°C. The fit was excellent and allows for the generation of a smooth CTE function, shown in Figure 4. The secant CTE is useful for engineering purposes and is defined as the effective CTE between a given temperature and room temperature.

Thermal Strain Measurements



Average CTE of Samples

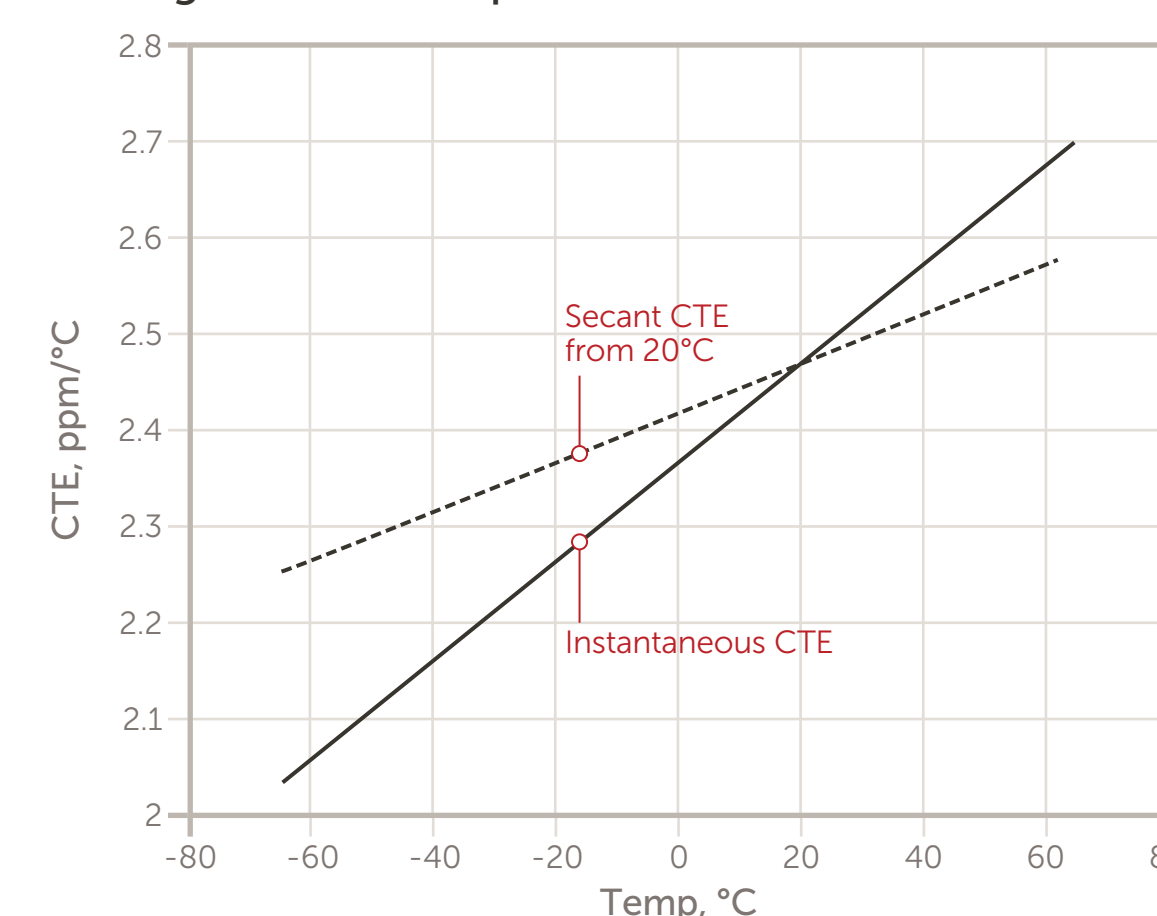


Figure 4. Thermal strain (left), CTE (right).

A polished cladding sample was interferometrically tested over temperature in a laboratory environment. The sample was placed on a hot plate with a thermocouple mounted on the edge to record temperature. Once the sample reached approximately 50°C, it was removed from the hotplate and placed in front of a 4D AccuFiz interferometer. As the sample cooled, ten interferograms were taken and averaged at each of five temperatures. The average of the measurements at the final temperature, 28°C, was used as a reference and subtracted from the measurements at the higher temperatures. The resulting error was predominately power, as expected, with the direction of the error consistent with a cladding CTE lower than the substrate CTE. At each temperature, the power term was fitted and plotted as shown in the right side of the figure. Those data points were fit with a line and that information was used to estimate the difference in CTE as described.

Next, a polished pathfinder mirror was tested at MIT LL interferometrically over temperature in a TVAC chamber. This mirror was clad and polished but without an optical coating. The mirror was fixtured such that the mirror bosses would sit in vee-grooves (Figure 5), with the mirror surface oriented such that the long dimension was aligned with gravity. A thin layer of Kapton was placed between the mirror bosses and the vee-grooves to minimize friction and avoid over-constraint. The mirror and fixture were placed in a cold box where the top and four lateral sides were conductively-coupled to a cold plate underneath the mirror.

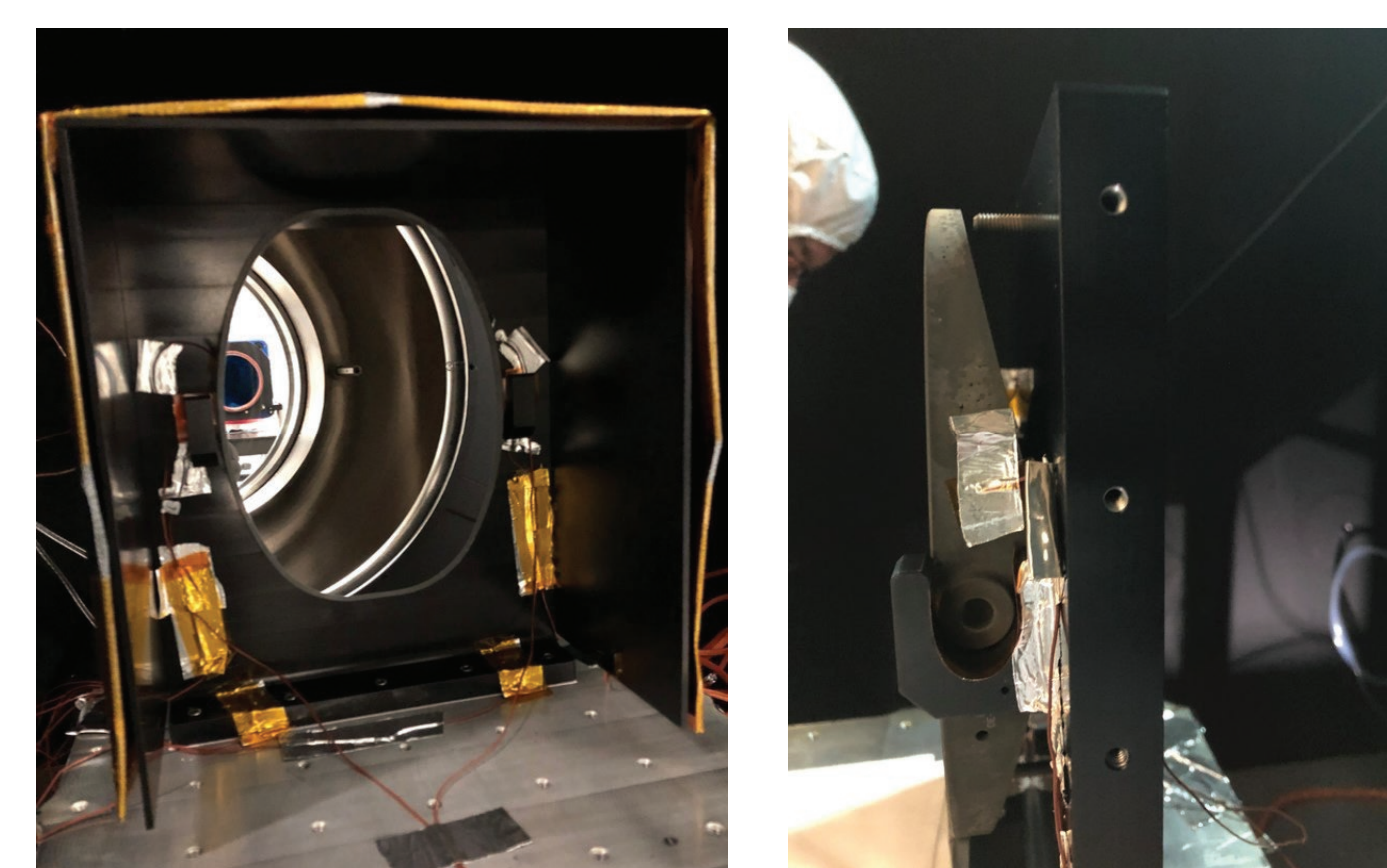


Figure 5. Pathfinder mirror in the TVAC fixture: mirror in cold box (left), mirror bosses in vee-grooves (right).

The cold plate was cooled to approximately -60°C to bring the mirror to a stable temperature of -38°C, which is the coldest operational mirror temperature expected on orbit. Optical measurements were taken with a 6-inch phase shift interferometer (AccuFIZ, 4D Technology Inc). Because the pathfinder had steep edge roll-off from polishing, a 130 mm mask was used to measure just the central portion of the mirror. Figure 6 shows the baseline ambient temperature along with interferograms from the cold temperatures. The results show the expected trend of a change in power from warm to cold. The mirror was becoming more convex, consistent with a cladding CTE slightly lower than the substrate CTE.

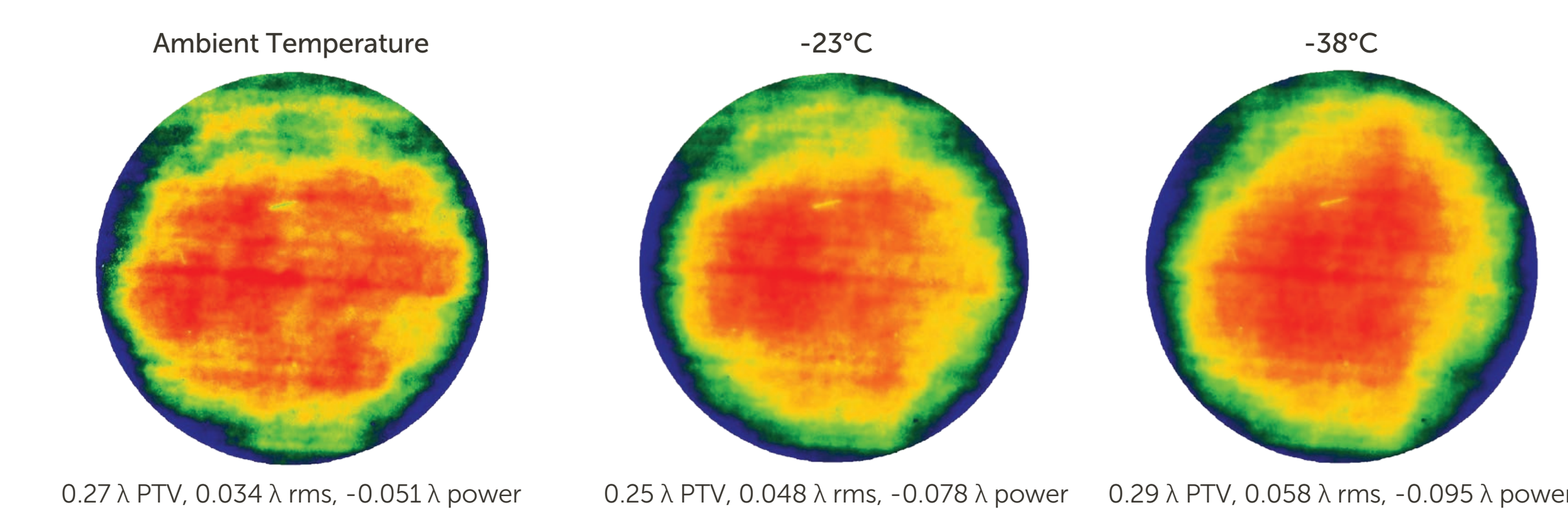


Figure 6. Pathfinder mirror reflected wavefront error in TVAC chamber at ambient and cold operational temperatures.

Entegris SUPERSiC-SP material was chosen to optimize performance. Material was characterized with CVD SiC coating, CTE impact to performance measured.

RESULTS

For purposes of determining the effect of the cladding, we are interested in comparing this measured CTE with published CTE data on CVD SiC. Li³ reports a CTE for CVD SiC that is plotted along with the TMA measurements from Section 3.1 in Figure 7. The comparison suggests a difference of approximately 0.25 ppm/°C at room temperature, growing larger at lower temperatures. It is unclear, however, how applicable the published CTE values for CVD SiC are to the Entegris cladding material, so this should be treated as only a first order estimate. The difference in CTE between the two materials can also be derived from the optical tests on the cladding disks. We can use a closed form solution to estimate the CTE difference based on the results of the cladding disks. Pepi⁴ describes a closed form expression relating sag Y to thermal strain for a clad disk given the geometry and material properties:

$$Y = \frac{3E_1\Delta\epsilon D^2 t(1 - \nu_2)}{4E_2 h^2(1 - \nu_1)} \quad (1)$$

where E_1 and E_2 , ν_1 and ν_2 are the elastic moduli and the Poisson's ratio of the substrate and the cladding respectively; D , t and h are the diameter, cladding thickness and total thickness of the disk. The term is the change in strain of the cladding with temperature and can be related to the difference in thermal expansion coefficient $\Delta\alpha$ and temperature T :

$$\Delta\epsilon = \Delta\alpha T \quad (2)$$

The curve in the coupon imposed between 38°C and 29°C is the change in sag as a function of temperature, so the slope of the line can be described as $S = Y/T$. Substituting S and equation 2 into equation 1 and solving for $\Delta\alpha$ yields:

$$\Delta\alpha = \frac{4E_2 S h^2 (1 - \nu_1)}{3D^2 E_1 t (1 - \nu_2)} \quad (3)$$

The pathfinder mirror originally had approximately 75 μ m of CVD deposited. It is estimated that about half of that was removed by surfacing and polishing the mirror, leaving an average thickness of 38 μ m. A finite element model (FEM) was constructed with solid tetrahedral elements modeling the bulk material and plate elements modeling the thin cladding. The cladding was assigned a CTE 0.14 ppm/K lower than the substrate material. A -60°C thermal soak was applied, representing the change from 22°C down to -38°C, and the surface deformation was processed over a 130 mm central section of the mirror to compare with test results. Figure 8 shows the FEM results compared with the test results.

CTE Comparison

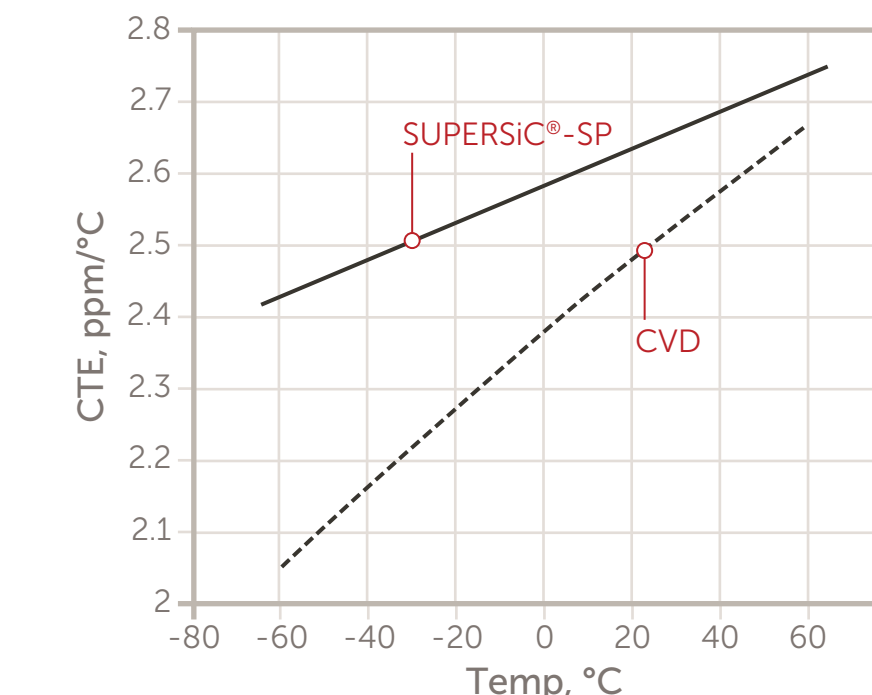


Figure 7. Comparison of SUPERSiC-SP and CVD thermal expansion coefficient.

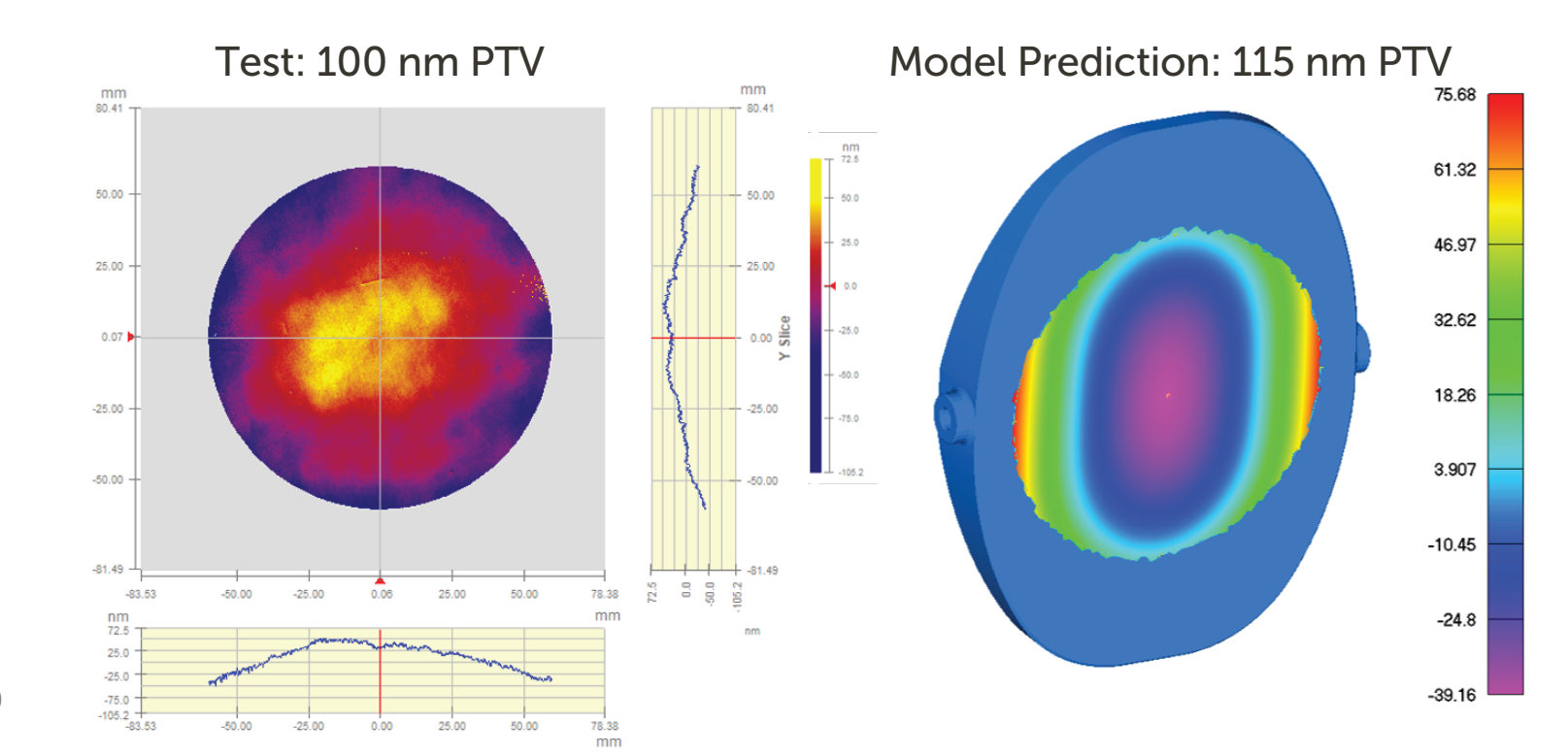


Figure 8. Test vs. analysis error from ambient to -38°C. Measured change in wavefront error (left) vs. FEM predicted error (right).

CONCLUSIONS

- CTE delta between SUPERSiC-SP and CVD SiC = 0.14 ppm/K
- Results are within expected range, linear from RT down to -40°C
- Authors suggest 0.2 ppm/K design and analysis criteria to account for uncertainty in coating thickness and measurement accuracy

The test results described in the analysis are all consistent in that they indicate the CTE of the deposited CVD SiC is slightly lower than the -SP substrate material. The magnitude of the difference derived from coupon testing is 0.14 ppm/K, but given the uncertainty in the cladding thickness for the measured samples and the uncertainty of the measurement itself, this should be considered an approximate value at or near room temperature. The usefulness of this result is evidenced by the reasonably good agreement between FEM results using this value and the TVAC test of the QZSS-HP pathfinder mirror. This result also suggests that the effect is approximately linear down to -40°C.

For future programs using the same materials and process, the authors suggest a slightly higher CTE difference of 0.2 ppm/K be assumed for analysis in the design phase. This will allow for a conservative budgeting of the error and accounts for the uncertainty in the results presented here.

QZSS platform satellites to launch in 2023–2024 using MIT SSA optical payload and Entegris SUPERSiC mirrors.

REFERENCES

- [1] Entegris, "2021 Scientific Report," PDF, 2021. <https://www.entegris.com/content/dam/web/resources/reports/scientific-report-2021-11637.pdf>. (Accessed: 22 April 2022).
- [2] D'Amico, G. C., "2021 Scientific Report," Research Gate, Thesis, 2015. https://www.researchgate.net/figure/Equilibrium-phase-diagram-of-the-carbon-silicon-system-167_fig10_301228848. (Accessed: 22 April 2022).
- [3] Li, B., "Pellet Cladding Mechanical Interactions of Ceramic Claddings Fuels Under LightWater Reactor Conditions," University Libraries, Master Thesis, 2013. <http://scholarcommons.sc.edu/etd/2366>. (Accessed: 22 April 2022).
- [4] Pepi, J. W., [Opto-Structural Analysis], SPIE, Bellingham, Washington (2018).